

AIAA'83



AIAA-83-0190

Design of Optimum Propellers

C.N. Adkins, Consulting Engineer, Falls Church, VA; and R.H. Liebeck, Douglas Aircraft Co., Long Beach, CA

AIAA 21st Aerospace Sciences Meeting

January 10-13, 1983/Reno, Nevada

DESIGN OF OPTIMUM PROPELLERS

Charles N. Adkins*
Falls Church, Virginia

and

Robert H. Liebeck**
Douglas Aircraft Company
Long Beach, California
and
University of Southern California
Los Angeles, California

Abstract

Improvements have been made in the equations and computational procedures for the design of propellers and wind turbines of maximum efficiency. These eliminate the small angle approximation and many of the "lightly loaded" approximations prevalent in the classical design theory. Though wake contraction is still neglected, certain viscous terms have been added to the induced velocities which are important at low Reynolds numbers or high profile drag. An iterative scheme is introduced for accurate calculation of the vortex displacement velocity and the flow angle distribution. Momentum losses due to radial flow can be estimated by either the Prandtl or Goldstein momentum loss function. For the less complex Prandtl function, the "lightly loaded" approximation can be eliminated for both design and analysis. The methods presented here now bring into exact agreement the procedures for design and analysis even when applied to cases of low Reynolds number and large disk loading. Furthermore, the exactness of this agreement makes possible an empirical verification of the Betz condition that a constant displacement velocity across the wake provides a design of maximum propeller efficiency.

| | | |
|------------|---|---|
| r | = | radial coordinate |
| T | = | thrust |
| T_c | = | thrust coefficient = $2 T / \rho V^2 \pi R^2$ |
| V | = | freestream velocity |
| v' | = | vortex displacement velocity |
| W | = | local total velocity |
| w_n | = | velocity normal to the vortex sheet |
| w_t | = | tangential (swirl) velocity |
| x | = | nondimensional distance = $\Omega r / V$ |
| α | = | angle of attack |
| β | = | blade twist angle |
| Γ | = | circulation |
| ϵ | = | drag to lift ratio |
| ζ | = | displacement velocity ratio = v' / V |
| η | = | propeller efficiency |
| λ | = | speed ratio = $V / \Omega R$ |
| ξ | = | nondimensional radius = $r / R = \lambda x$ |
| ξ_0 | = | nondimensional hub radius |
| ξ_e | = | nondimensional Prandtl radius |
| ρ | = | fluid density |
| σ | = | local solidity = $Bc / 2 \pi r$ |
| ϕ | = | flow angle |
| ϕ_t | = | flow angle at the tip |
| Ω | = | propeller angular velocity |

Superscripts

' (prime) = derivative with respect to r or ξ , unless otherwise noted

Nomenclature

| | | |
|-------|---|--|
| a | = | axial interference factor |
| a' | = | rotational interference factor |
| B | = | number of blades |
| b | = | axial slipstream factor |
| c | = | blade section chord |
| C_d | = | blade section drag coefficient |
| C_l | = | blade section lift coefficient |
| C_p | = | power coefficient = $P / \rho n^3 D^5$ |
| C_T | = | thrust coefficient = $T / \rho n^2 D^4$ |
| C_x | = | torque force coefficient |
| C_y | = | thrust force coefficient |
| D | = | propeller diameter = $2R$ |
| D' | = | drag force per unit radius |
| F | = | Prandtl momentum loss factor |
| G | = | circulation function |
| J | = | advance ratio = V / nD |
| L' | = | lift force per unit radius |
| n | = | propeller revolutions per second |
| P | = | power into propeller |
| P_c | = | power coefficient = $2 P / \rho V^3 \pi R^2$ |
| Q | = | torque |
| R | = | propeller tip radius |

Introduction

In 1936, a classic treatise on propeller theory was authored by H. Glauert.¹ Here a combination of momentum theory and blade element theory, when corrected for momentum loss due to radial flow, provide a good method for analysis of arbitrary designs even though contraction of the propeller wake is neglected. Though the theory is developed for low disk loading (small thrust or power per unit disk area) it works quite well for moderate loading and, in light of its simplicity, is adequate for estimating performance even for high disk loadings. The conditions under which a design would have minimum energy loss were stated by A. Betz² as early as 1919, however, no organized procedure for producing such a design is evident in Glauert's work. Those equations which are given make extensive use of small angle approximations and relations applicable only to light loading conditions. The momentum blade element theory for analysis took several decades to become generally accepted only as blade section data and propeller test procedures became sufficiently accurate to validate its usefulness. But the design equations, in their rudimentary form, laid fallow for more decades still, yielding to experiment and experience for the creation of new designs.

* Consulting Engineer

Member AIAA

**Principal Engineer, Aerodynamics Subdivision
Professor, Aerospace Engineering Department
Associate Fellow AIAA

Quite recently (1979), E. Larrabee³ resurrected the design equations and presented a straightforward procedure for optimum design. However, there are still three problems: first, small angle approximations are used; second, the solution for the displacement velocity is accurate only for vanishingly small values (light loading), though an approximate correction is suggested for moderate loading; and third, there are viscous terms missing in the expressions for the induced velocities. The purpose of this paper is to correct these difficulties and bring the design method into exact agreement with that of analysis. With this done, it is now possible to verify empirically the optimality of design.

The Momentum Equations

Detailed axial and general momentum theory is described by Glauert¹, and only a brief summary is given here to point out several important features. Consider a fluid element of mass dm far upstream moving toward the propeller disk in a thin annular stream tube with velocity V . It arrives at the disk with increased velocity $V(1+a)$, where a is called the axial interference factor. At the disk, dm exist in the annulus $2\pi r dr$ and the mass rate per unit radius passing through the disk is $2\pi r \rho V(1+a)$, neglecting radial flow. The element dm moves downstream into the far wake increasing speed to the value $V(1+b)$, where b is called the axial slipstream factor. Axial momentum theory determines b to be exactly $2a$, whereas the general theory (which includes rotation of the flow) determines b to be approximately $2a$. Using the axial approximation, which is generally accepted, the overall change in momentum of the element is $2VaF dm$ where F , the momentum loss factor, accounts for radial flow of the fluid. The thrust per unit radius T' acting on the annulus can now be expressed as

$$T' = dT/dr = 2\pi r \rho V(1+a)(2VaF) \quad (1a)$$

By similar arguments, the torque per unit radius Q' is given by

$$Q'/r = 2\pi r \rho V(1+a)(2\Omega r a' F) \quad (1b)$$

where Ω is the angular velocity of the propeller and a' is called the rotational interference factor. Flow geometry about a blade element at the disk is shown in Figure 1, where the total local velocity W acts on the blade element with

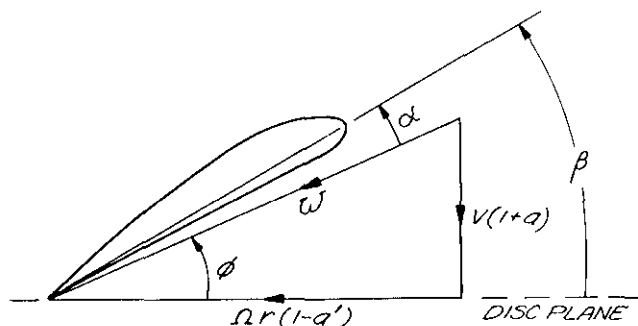


Fig. 1 Flow geometry for blade element at radial station r .

angle of attack α and acts on the disk at the flow angle ϕ . The momentum loss factor F goes from about 1 at the hub (where the radial flow is typically negligible), to zero at the tip, and is not unlike the spanwise loading of a wing. The functional form of this factor was first estimated by Prandtl^{1,2}, and a more accurate (though more complex) form was determined by Goldstein⁴ and Lock.^{5,6,7}

The Circulation Equations

At each radial position along the blade, infinitesimal vortices are shed and move aft as a helicoidal vortex sheet. Since these vortices follow the direction of local flow, the helix angle of the spiral surface is the flow angle ϕ shown in Figure 1. The Betz condition for minimum energy loss, neglecting contraction of the wake, is for the vortex sheet to be a regular screw surface; i.e. $r \tan \phi$ must be a constant independent of radius. This optimum vortex sheet acts as an Archimedean screw, pumping fluid aft between rigid spiral surfaces.

At the blade station r , the total lift per unit radius is given by

$$L' = dL/dr = B \rho W \Gamma \quad (2)$$

and in the wake, the circulation in the corresponding annulus is

$$B \Gamma = 2\pi r F w_t \quad (3)$$

where w_t is the local tangential velocity in the wake and B is the number of blades. Setting the circulation Γ in (2) equal to that in (3) will ultimately determine that circulation distribution $\Gamma(r)$ which minimizes the induced power of the propeller.

In order to obtain $\Gamma(r)$, it is necessary to relate w_t to a more measurable quantity. Figure 2 shows the wake vortex filament at station r and the definition of the various velocity components there. The motion of the fluid must be normal to the local vortex sheet, and this normal velocity is called w_n . Therefore, the tangential velocity is given by

$$w_t = w_n \sin \phi$$

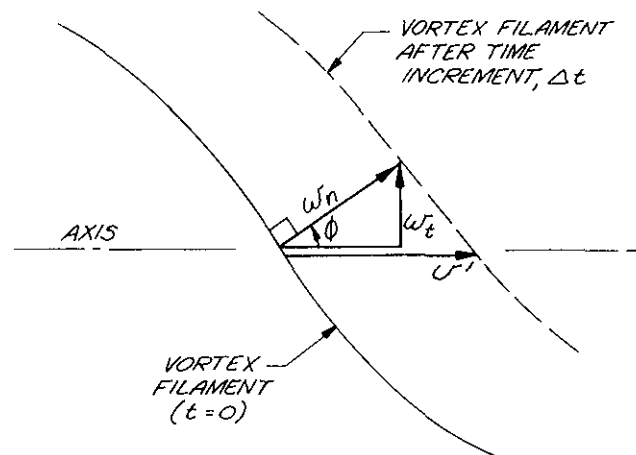


Fig. 2 Definition of the displacement velocity v' in the propeller wake.

However, for a coordinate system fixed to the propeller disk, the axial velocity of the vortex filament would be

$$v' = w_n / \cos \phi$$

where the increase in magnitude of v' over w_n is due to rotation of the filament. This is analogous to a barber pole where it appears that the stripes are translating in spite of the fact that only a rotational velocity exists. It will become clear that it is convenient to use the vortex displacement velocity v' and the corresponding displacement velocity ratio $\zeta = v'/V$. The tangential velocity is then

$$w_t = V \zeta \sin \phi \cos \phi$$

and the circulation of (3) can be expressed as

$$\Gamma = 2 \pi V^2 \zeta G / (B \Omega) \quad (4)$$

where G is the circulation function

$$G = F \times \cos \phi \sin \phi \quad (5)$$

and x is the speed ratio given by

$$x = \Omega r / V.$$

The circulation equations for thrust T' and torque Q' per unit radius can be written by inspection of Figure 3 as

$$\begin{aligned} T' &= L' \cos \phi - D' \sin \phi \\ &= L' \cos \phi (1 - \epsilon \tan \phi) \end{aligned} \quad (6a)$$

$$\begin{aligned} Q'/r &= L' \sin \phi + D' \cos \phi \\ &= L' \sin \phi (1 + \epsilon / \tan \phi) \end{aligned} \quad (6b)$$

where ϵ is the drag-to-lift-ratio of the blade element. Next, using (2), the lift per unit radius L' can be replaced by $\Gamma(r)$ which in turn is related to conditions in the wake by (3). Based on the flow in the wake, $\Gamma(r)$ is given by (4) and (5), and T' and Q'/r are reduced to being functions of ϕ and the displacement velocity $\zeta = v'/V$. The local flow angle ϕ will clearly be a function of the radius; however, at this stage of the analysis, the optimum distribution $\zeta(r)$ is not yet determined. Several diagrams and an excellent photograph of the vortex sheet can be found in Reference 8.

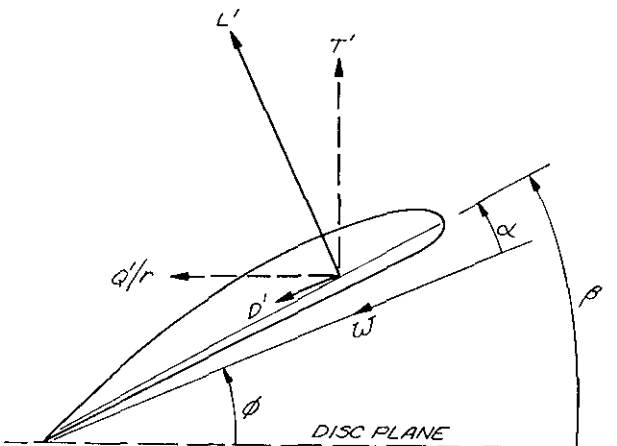


Fig. 3 Force diagram for a blade element.

The Condition for Minimum Energy Loss

At this point, a departure from Larrabee's³ design procedure is made, and the momentum equation (1) and the circulating equations (6) are required to be exactly equal. This condition results in the interference factors being related to the displacement velocity ratio ζ by the equations

$$a = (\zeta/2) \cos^2 \phi (1 - \epsilon \tan \phi) \quad (7a)$$

$$a' = (\zeta/2x) \cos \phi \sin \phi (1 + \epsilon / \tan \phi) \quad (7b)$$

where the terms in epsilon correctly describe the viscous contribution. Equations (7), together with the geometry of Figure 1, lead to the very important simple relation

$$\tan \phi = (1 + \zeta/2)/x = (1 + \zeta/2)\lambda/\xi \quad (8)$$

Here, λ is the speed ratio $V/\Omega R$ (a constant) and ξ is the nondimensional radius r/R which varies from ξ_0 at the hub to unity at the edge of the disk. The relation between the two nondimensional distances and the constant speed ratio is

$$x = \Omega r / V = (r/R)/\lambda = \xi/\lambda.$$

Recalling the Betz condition, $r \tan \phi = \text{constant}$, (8) proves that in order for the vortex sheet to be a regular screw surface, the displacement velocity ζ must be a constant independent of radius, and this then is the condition for minimum energy loss.

The Constraint Equations

For design, it is necessary to specify either the thrust T delivered by the propeller or the power P delivered to the propeller. The nondimensional thrust and power coefficients used for design are

$$T_C = 2 T / (\rho V^2 \pi R^2) \quad (9a)$$

$$\begin{aligned} P_C &= 2 P / (\rho V^3 \pi R^2) \\ &= 2 Q \Omega / (\rho V^3 \pi R^2) \end{aligned} \quad (9b)$$

and using these definitions, (6) can be written as

$$T'_C = I'_1 \zeta - I'_2 \zeta^2 \quad (10a)$$

$$P'_C = J'_1 \zeta + J'_2 \zeta^2 \quad (10b)$$

where the primes denote derivatives with respect to ξ , and

$$I'_1 = 4 \xi G (1 - \epsilon \tan \phi) \quad (11a)$$

$$I'_2 = \lambda (I'_1/2 \xi) (1 + \epsilon / \tan \phi) \sin \phi \cos \phi \quad (11b)$$

$$J'_1 = 4 \xi G (1 + \epsilon / \tan \phi) \quad (11c)$$

$$J'_2 = (J'_1/2) (1 - \epsilon \tan \phi) \cos^2 \phi \quad (11d)$$

Since ζ is constant for an optimum design, a specified thrust gives the constraint equations

$$\zeta = (I_1/2 I_2) - [(I_1/2 I_2)^2 - T_C/I_2]^{1/2} \quad (12)$$

$$P_C = J_1 \zeta + J_2 \zeta^2 \quad (13)$$

Similarly, if power is specified, the constraint relations are

$$\zeta = -(J_1/2 J_2) + [(J_1/2 J_2)^2 + P_C/J_2]^{1/2} \quad (14)$$

$$T_C = I_1 \zeta - I_2 \zeta^2 \quad (15)$$

where the integration has been carried out over the region $\xi = \xi_0$ to $\xi = 1$.

Blade Geometry

In the element dr of a single blade, let c be the chord and C_L the local lift coefficient. Then, the lift per unit radius of one blade is

$$\rho W^2 c C_L/2 = \rho W \Gamma$$

where Γ is given by (4). It follows directly that

$$Wc = 4 \pi \lambda G V R \zeta / (C_L B). \quad (16)$$

Assume for the moment that the constant displacement velocity ζ is known, then the local value of ϕ is known from (8) and the above relation is a function only of the local lift coefficient. Since the local Reynolds number is Wc divided by the kinematic viscosity, (16) plus a choice for C_L will determine the Reynolds number and also the drag-to-lift ratio ϵ from the airfoil section data. The total velocity is then determined by Figure 1 as

$$W = V(1 + a)/\sin\phi \quad (17)$$

where a is given by (7), and the chord is then known from (16). If the choice for C_L causes ϵ to be a minimum, then viscous as well as momentum losses will be minimized, and overall propeller efficiency will be the highest possible value. If the blade strength is found to be insufficient at the hub, C_L can be reduced to increase the chord, or a thicker section can be used in that region. For preliminary considerations, it is usually sufficient to choose one C_L , the design C_L , for determining blade geometry. Since angle of attack α is known from C_L and Reynolds number, the blade twist with respect to the disk is $\beta = \alpha + \phi$. G is zero at the edge of the disk, and therefore the tip chord is always zero for a finite lift coefficient.

The Design Procedure

Either the Prandtl or Goldstein relation for the momentum loss function F can be selected. For simplicity, only the Prandtl relation is described as

$$F = (2/\pi) \arccos(e^{-f})^* \quad (18)$$

*For computational purposes, the form $F = (2/\pi) \arctan[(e^{2f} - 1)^{1/2}]$ is more tractable.

where

$$f = (B/2)(1 - \xi)/\sin\phi_t \quad (19)$$

and ϕ_t is the flow angle at the tip. From (8)

$$\tan\phi_t = \lambda (1 + \zeta/2) \quad (20)$$

so that a choice for ζ determines the function F as well as ϕ by

$$\tan\phi = (\tan\phi_t)/\xi \quad (21)$$

which is simply the condition that the vortex sheet in the wake is a rigid screw surface ($r \tan\phi = \text{constant}$).

Next, an initial estimate for the displacement velocity ratio is chosen as either zero, the lightly loaded approximation, or by the estimate

$$\zeta \approx 0.5 P_C / (\xi_e^2 - \xi_0^2) \approx 0.5 T_C / (\xi_e^2 - \xi_0^2)$$

where ξ_0 is the nondimensional hub-radius and ξ_e is the effective Prandtl radius given by

$$\xi_e \approx 1 - 1.386 \lambda/B.$$

A nonzero estimate for ζ will only reduce computational time, not accuracy.

The design is initiated with the specified conditions of power (or thrust), hub and tip radius, rotational rate, freestream velocity, number of blades, and a finite number of stations at which blade geometry is to be determined. Also, the design lift coefficient, one for each station, if it is not constant, must be specified. The design procedure can then be described by the following steps:

1. Select an initial estimate for ζ ($\zeta = 0$ will work).
2. Determine the values for F and ϕ at each blade station by (18-21).
3. Determine Wc and Reynolds number from (16).
4. Determine ϵ and α from airfoil section data.
5. If ϵ is to be minimized, change C_L and repeat steps 3 and 4 until this is accomplished at each station.
6. Determine a and a' from (7) and W from (17).
7. Compute the chord from step 3 and the blade twist $\beta = \alpha + \phi$.
8. Determine the four derivatives in I and J from (11) and numerically integrate these from $\xi = \xi_0$ to $\xi = 1$.
9. Determine ζ and P_C from (12-13), or ζ and T_C from (14-15).
10. If this new value for ζ is not sufficiently close to the old one (say, within 0.1%) start over at step 2 using the new ζ .
11. Determine propeller efficiency as T_C/P_C , and other features such as solidity, etc.

The above steps converge rapidly with a direct substitution for ζ , seldom taking more than three trials. An accurate description of viscous losses can be obtained by performing a second design with ϵ equal to zero and noting the difference in propeller efficiency.

Analysis of Arbitrary Designs

The analysis method is outlined here in order to discuss problems of convergence for off design and for square-tipped propellers in general, and to point out two minor errors in Glauert's work. Figure 4 (which is simply an alternate version of Figure 3) shows the relation between the propeller force coefficients C_y and C_x and the airfoil coefficients C_l and C_d . The equations are

$$C_y = C_l \cos\phi - C_d \sin\phi$$

$$C_x = C_l \sin\phi + C_d \cos\phi$$

and the relations for the thrust T' and torque Q' per unit radius are then

$$T' = (1/2) \rho W^2 Bc C_y \quad (22a)$$

$$Q'/r = (1/2) \rho W^2 Bc C_x \quad (22b)$$

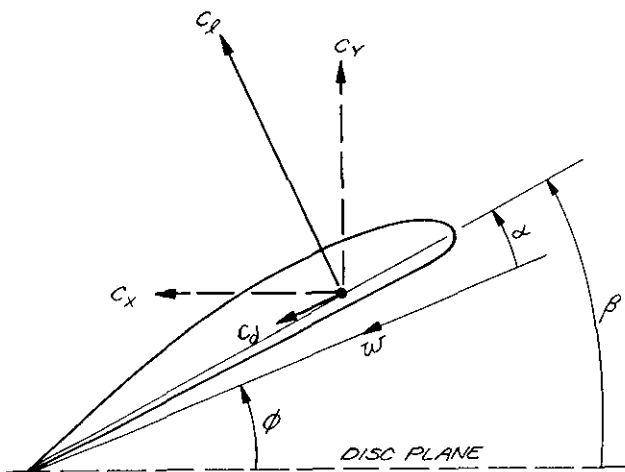


Fig. 4 Force coefficients for propeller blade element analysis.

Again, it is required that the loading (22) be exactly equal to the momentum result (1). With the use of the flow geometry in Figure 1, this requires the interference factors to be

$$a = \sigma K / (F - \sigma K) \quad (23a)$$

$$a' = \sigma K' / (F + \sigma K') \quad (23b)$$

where

$$K = C_y / (4 \sin^2\phi) \quad (24a)$$

$$K' = C_x / (4 \cos\phi \sin\phi) \quad (24b)$$

and σ is the local solidity given by

$$\sigma = Bc / (2 \pi r).$$

Equations (23) correct the placement of the factor F used by Glauert in his Equations (5.5) of Chapter VII as identified by Larrabee.³

The relation for the flow angle is obtained from Figure 1 and (23) as

$$\tan\phi = [V(1+a)] / [\Omega r(1-a')]. \quad (25)$$

For determining the function F in (18), Glauert suggests the relation $\sin\phi_t = \xi \sin\phi$ for use in (19). It is recommended that (21) be used instead, i.e.

$$\tan\phi_t = \xi \tan\phi$$

which is exact for the analysis of an optimally designed propeller at the design point.

The analysis procedure requires an iterative solution for the flow angle ϕ at each radial position ξ . An initial estimate for ϕ can be obtained from (8) by setting ζ equal to zero. Since the blade twist β is known, the value for α in Figure 3 is $\beta - \phi$ and the airfoil coefficients are known from the section data. The Reynolds number is determined from the known chord and the total velocity W which is obtained from Figure 1 and (23a), and the new estimate for ϕ is then found from (25). A direct substitution of the new ϕ for the old value will cause adequate convergence for an optimum design which is being analyzed at the design point. However, for analysis off design and for non-optimum designs, some combination of the old and new values for ϕ is required to cause adequate convergence. Under some conditions (usually near the tip) convergence may not be possible at all due to large values for the interference factors a and a' in (23). Since F is zero at the tip and σ is not, for a square tip propeller, the value for a is -1 and a' is $+1$. Such values are physically impossible since the slipstream factors are approximately twice the values at the rotor plane. Wilson and Lissaman⁹ suggest empirical relations for resolving this problem, whereas Viterna and Janetzke¹⁰ give empirical arguments for clipping the magnitude of a and a' at the value 0.7 (σ/F at the tip is finite at the design point for an optimum propeller).

For analysis, the conventional thrust and power coefficients are

$$C_T = T / (\rho n^2 D^4)$$

$$C_P = P / (\rho n^3 D^5)$$

where n is revolutions per second and D is the propeller diameter. Using (22) and (24), the differential forms, with respect to ξ , are given by

$$C_T' = (\pi^3/4) \sigma C_y \xi^3 F^2 / [(F + \sigma K') \cos\phi]^2$$

$$C_P' = C_T' \pi \xi C_x / C_y.$$

When these have been integrated from the hub to the tip, the propeller efficiency is

$$\eta = C_T J / C_P$$

where $J = V / (nD)$ is the advance-diameter ratio.

Propeller performance is typically described by plots of C_T , C_p , and η vs. J .

Airfoil Section Data

In the previous discussions, reference has been made to the use of airfoil characteristics in the form of lift curves and drag polars. This data should include a reliable estimate of the drag variation with respect to Reynolds number over that range in which the propeller is expected to operate. In addition, a detailed knowledge of the airfoil's post-stall behavior up to an angle of attack of 90 degrees is essential for predicting off-design performance, particularly in the case of wind turbines. Such data may be difficult to obtain; however, its importance should not be underestimated.

Empirical Optimality

In Chapter VII of Glauert's work, his equation (2.20) shows that when blade friction is neglected the most favorable distribution of circulation is one where the displacement velocity is constant across the wake. Here, the term $x^2/(1+x^2)$ is the small angle approximation of the circulation function G given by (5) of this paper. The effect of profile drag is shown by Glauert in his equation (3.5) which states that the optimum distribution for the displacement velocity ratio is

$$\zeta = \zeta_0 - \varepsilon x \quad (26)$$

where the effect of profile drag on thrust has been ignored. In order to study this problem empirically, consider a general function $H(x)$ and the two first-order terms of its Laurent series, $1/x$ and x , and describe the displacement velocity distribution as

$$\zeta = \zeta_0 + \delta_1 x + \delta_2/x \quad (27)$$

which includes the case of (26). It is desired to find values for δ_1 and δ_2 which maximize propeller efficiency subject to the constraints of (10). To solve this problem, ζ in (10) is replaced by (27). Then, a choice for δ_1 and δ_2 will enable a determination of ζ_0 and a calculation of overall propeller efficiency. A systematic study of various propeller conditions was undertaken using the design/analysis procedures of this paper. Under no conditions could nonzero values for δ_1 and δ_2 be found which caused an increase in propeller efficiency. Therefore, it was concluded that a constant displacement velocity is at least locally optimum whether profile drag is considered or not. The momentum and viscous losses are then uncoupled; the former is minimized by constant displacement velocity, the latter by choosing a C_d -distribution so that the drag-lift ratio is everywhere a minimum.

Windmills

All of the analyses described in this paper are directly applicable to the windmill problem after a minor adjustment in the angle definitions of Figure 1. The corresponding flow geometry for a windmill is shown in Figure 5, where the primary distinction is that the blade section is inverted

(as compared with a propeller), and the local angle of attack is measured from below the local velocity vector. Corresponding relations for the angles are:

$$\begin{array}{ll} \text{windmill} & \alpha \approx \phi - \beta \\ \text{propeller} & \alpha \approx \beta - \phi \end{array}$$

as shown in Figures 5 and 1, respectively. Referring again to Figures 1 and 5, C_d for the windmill is negative with respect to that for the propeller, and this sign change together with the angle definition will convert the propeller methods to the windmill application. For the design case, the input P_c value should be negative, and the resulting values of v' (and the interference factors a and a') and T_c will also be negative. (Thrust is of less interest for a windmill since it typically represents the tower load and is not a main performance parameter.) Similarly, the analysis results for a windmill rotor will yield negative values for both P_c and T_c .

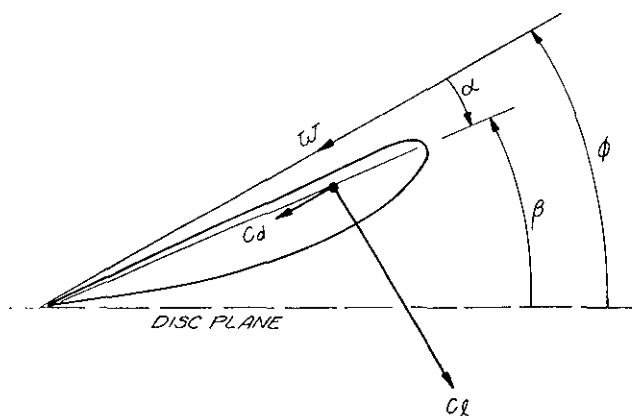


Fig. 5 Force coefficients for windmill blade element.

Example

As a sample calculation, the design of a propeller for a light airplane is considered, where the design conditions are:

| | |
|-------------|---------------------|
| hp = 70 | no. of blades = 2 |
| rpm = 2400 | tip dia. = 5.75 ft. |
| V = 110 mph | hub dia. = 1.00 ft. |
| J = 0.7 | NACA 4415 airfoil |

The resulting design is described in Table I which gives for each radial station: blade chord, blade pitch angle, local flow angle, blade loading, blade section lift to drag ratio, local Reynolds number, local Mach number, and the interference coefficients a and a' .

This propeller geometry has in turn been analyzed at the design condition and the result is given in Table II. Agreement is virtually exact. Analysis over a range of values of the advance ratio $J = V/(nD)$ provides the typical propeller performance plots which are shown in Figure 6, and Figure 7 gives the blade lift coefficient distribution over a range of J 's where the design condition is the $C_d = 0.7 = \text{constant}$ line at $J = 0.7$.

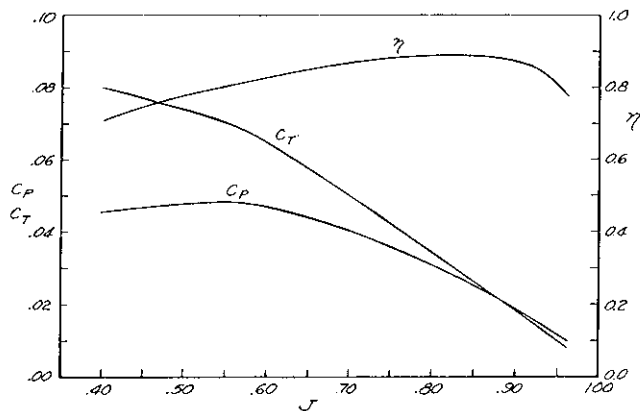


Fig. 6 Analysis results for propeller with $C_L = 0.7 = \text{constant}$ at the design condition.

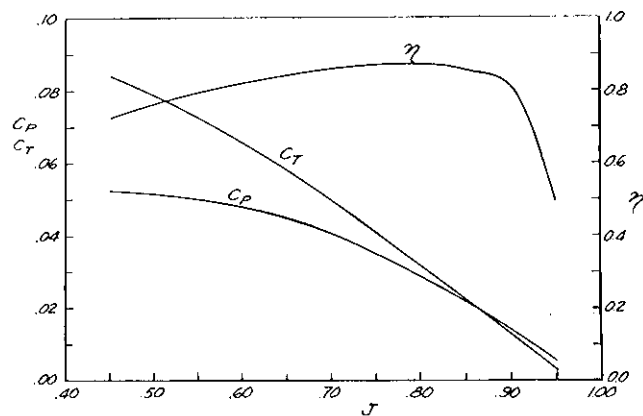


Fig. 8 Analysis results for propeller with chord = 4 in. = constant.

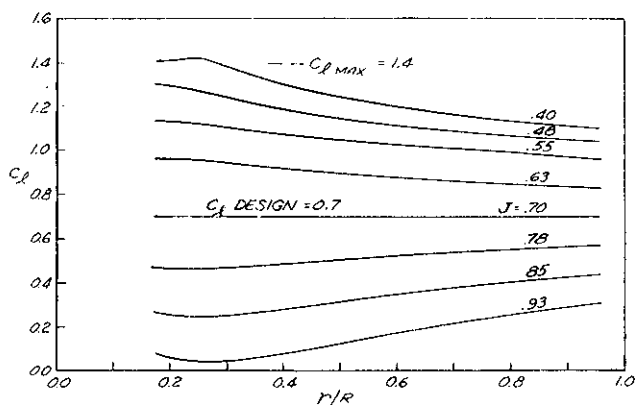


Fig. 7 Blade section C_L variation for $C_L = 0.7 = \text{constant}$ at the design condition.

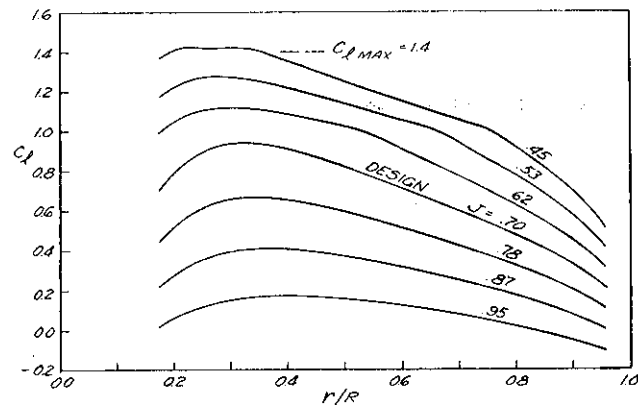


Fig. 9 Blade section C_L variation for propeller with chord = 4 in. = constant.

The effect of variations in the design conditions can be readily evaluated. If, for example, the blade chord is held constant (which requires that the local blade C_L varies as required by the optimum blade loading) the resulting performance is given in Figure 8. At the design point, the efficiency is only slightly reduced as compared with the constant C_L design; however, the range of J over which the efficiency remains high is reduced for the constant chord design. The corresponding blade C_L -distributions are shown in Figure 9 which indicates a wide range of local C_L 's at all values of J . This explains the reduced operational J -range since either the tip or the root of the blade quits "working" sooner than in the constant C_L design.

Another interesting result is obtained by varying the design C_L value, and the resulting performance for propeller designs for $C_L = 0.5$ and $C_L = 0.9$ is compared with that for $C_L = 0.7$ in Figure 10. The efficiency is seen to increase with increasing C_L ; however the blade chord, and consequently the blade thickness for a given airfoil section, is reduced since the blade loading $c C_L$ is effectively the same for all three cases. Structural and other practical considerations will of course influence the choice of design C_L , particularly near the hub.

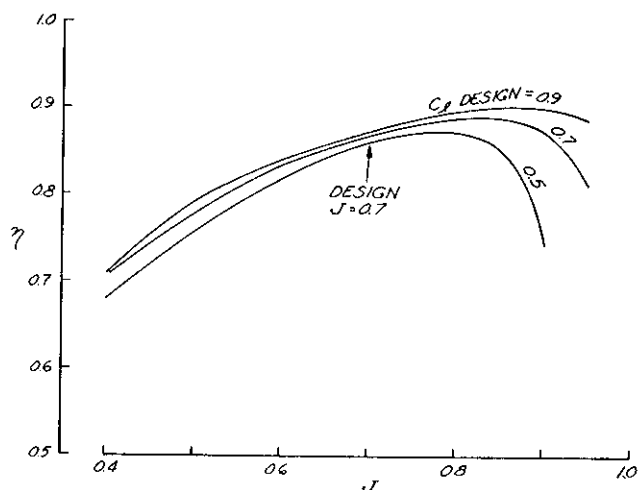


Fig. 10 Comparison of efficiencies of three propeller designs with design blade section lift coefficients of 0.5, 0.7, and 0.9.

Conclusions & Recommendations

The propeller theory of Glauert has been extended to improve the design of optimal propellers and refine the calculation of the performance of arbitrary propellers. Extensions of the theory include:

- a) Elimination of the light loading and small angle assumptions in the optimal design theory.
- b) Accurate calculation of the vortex displacement velocity which properly accounts for the blade section drag.
- c) Elimination of the light loading and small angle assumptions in the Prandtl momentum loss function for both design and analysis.

Implementation of these extensions has brought the design and analysis procedures to exact numerical agreement within the precision of computer analysis.

The primary approximation remaining in both procedures is the use of the axial momentum equations which require the increase in wake velocities to be twice those at the disk. Under certain conditions this approximation is not good and gives rise to the unnatural conditions and convergence problems described in the analysis section. It is suggested that improvements could be made by replacing the axial momentum equations with relations more closely aligned with the general theory, particularly in those differential stream tubes in which "heavy loading" exists. Such conditions appear to be more prevalent in the analyses at off design than in the design itself and, when combined with post stall misknowledge, can lead to large analysis errors. However, for design and analysis within the conventional operating regime, both procedures are simple, accurate, and reliable.

Acknowledgement

The authors would like to acknowledge Mr. D.N. Smyth of Douglas for his helpful ideas and suggestions, and Mr. P.P. Camacho of Douglas for his development of the computer code used in the calculations.

References

1. Glauert, H., "Airplane Propellers," Ed. by Durand, W., Aerodynamic Theory, Div. L, Vol. 4, Peter Smith, Gloucester, MA, 1976, pp. 169-269.
2. Betz, A., with appendix by Prandtl, L., "Screw Propellers with Minimum Energy Loss," Göttinger Reports, 1919, pp. 193-213.
3. Larrabee, E., "Practical Design of Minimum Induced Loss Propellers," SAE, pre-print for the April 1979 Business Aircraft Meeting and Exposition, Wichita, KS.
4. Goldstein, S., "On the Vortex Theory of Screw Propellers," Royal Society Proc., Series A, Vol. 123, London, 1929, pp. 440-465.
5. Lock, C., "The Application of Goldstein's Airscrew Theory to Design," British Aeronautical Research Committee, R. and M. 1377, Nov. 1930.
6. Lock, C., "An Application of Prandtl's Theory to an Airscrew," British Aeronautical Research Committee, R. and M. 1521, Aug. 1932.
7. Lock, C., "Tables for use in an Empirical Method of Airscrew Strip Theory Calculations," British Aeronautical Research Committee, R. and M. 1674, Oct. 1934,
8. Larrabee, E., "The Screw Propeller," Scientific American, Vol. 243, No. 1, July 1980, pp. 134-148.
9. Willson, R. and Lissaman, P., "Applied Aerodynamics of Wind Power Machines," Oregon State University, NSF/RA/N-74-113, PB-238595/3, July 1974.
10. Viterna, A. and Janetzke, D., "Theoretical and Experimental Power from Large Horizontal-Axis Wind Turbines," Proceedings from the Large Horizontal-Axis Wind Turbine Conference, DOE/NASA-LeRC, July 1981.

Table I Example propeller design.

| | | | | |
|---------------|-----------|-----------------|--------------|------------------|
| V = 161.33 | DT = 5.75 | BHP = 70.00 | CP = 0.0402 | SOLIDITY = 0.058 |
| RPM = 2400.00 | DM = 1.00 | THRUST = 207.44 | CT = 0.0498 | AF = 113.92 |
| J = 0.701 | B = 2 | ALT = 0.0 | ETA = 0.8693 | VP = 0.2046 |

DEFINING AIRFOIL: NACA 4415

CL = 0.7000

| I | R | CHORD | BETA | PHI | CCL | L/D | RN | MACH | A | AP |
|----|------|--------|-------|-------|--------|-------|------|------|--------|--------|
| 1 | 0.50 | 0.3353 | 56.42 | 54.75 | 0.2347 | 59.56 | 0.44 | 0.18 | 0.0333 | 0.0626 |
| 2 | 0.62 | 0.3966 | 50.50 | 48.83 | 0.2776 | 64.02 | 0.56 | 0.20 | 0.0435 | 0.0533 |
| 3 | 0.74 | 0.4325 | 45.48 | 43.81 | 0.3028 | 67.41 | 0.67 | 0.22 | 0.0525 | 0.0452 |
| 4 | 0.86 | 0.4484 | 41.24 | 39.57 | 0.3139 | 69.92 | 0.77 | 0.24 | 0.0601 | 0.0383 |
| 5 | 0.97 | 0.4501 | 37.64 | 35.97 | 0.3151 | 71.78 | 0.84 | 0.26 | 0.0663 | 0.0326 |
| 6 | 1.09 | 0.4423 | 34.57 | 32.90 | 0.3096 | 73.15 | 0.90 | 0.29 | 0.0715 | 0.0280 |
| 7 | 1.21 | 0.4285 | 31.94 | 30.27 | 0.3000 | 74.15 | 0.94 | 0.31 | 0.0757 | 0.0241 |
| 8 | 1.33 | 0.4110 | 29.66 | 27.99 | 0.2877 | 74.85 | 0.97 | 0.33 | 0.0792 | 0.0210 |
| 9 | 1.45 | 0.3913 | 27.68 | 26.01 | 0.2739 | 75.32 | 0.99 | 0.36 | 0.0821 | 0.0183 |
| 10 | 1.57 | 0.3704 | 25.95 | 24.28 | 0.2593 | 75.56 | 1.00 | 0.38 | 0.0845 | 0.0162 |
| 11 | 1.69 | 0.3487 | 24.42 | 22.75 | 0.2441 | 75.61 | 1.01 | 0.41 | 0.0865 | 0.0143 |
| 12 | 1.81 | 0.3265 | 23.06 | 21.39 | 0.2286 | 75.51 | 1.00 | 0.43 | 0.0882 | 0.0128 |
| 13 | 1.92 | 0.3040 | 21.85 | 20.18 | 0.2128 | 75.19 | 0.99 | 0.46 | 0.0897 | 0.0114 |
| 14 | 2.04 | 0.2810 | 20.77 | 19.10 | 0.1967 | 74.66 | 0.96 | 0.48 | 0.0909 | 0.0103 |
| 15 | 2.16 | 0.2572 | 19.79 | 18.12 | 0.1800 | 73.88 | 0.93 | 0.51 | 0.0920 | 0.0093 |
| 16 | 2.28 | 0.2324 | 18.90 | 17.23 | 0.1627 | 72.78 | 0.88 | 0.53 | 0.0929 | 0.0085 |
| 17 | 2.40 | 0.2059 | 18.10 | 16.43 | 0.1441 | 71.24 | 0.82 | 0.56 | 0.0937 | 0.0078 |
| 18 | 2.52 | 0.1768 | 17.36 | 15.69 | 0.1238 | 69.08 | 0.73 | 0.58 | 0.0945 | 0.0071 |
| 19 | 2.64 | 0.1433 | 16.69 | 15.02 | 0.1003 | 65.83 | 0.62 | 0.61 | 0.0951 | 0.0066 |
| 20 | 2.76 | 0.1006 | 16.07 | 14.40 | 0.0704 | 60.27 | 0.45 | 0.64 | 0.0956 | 0.0061 |
| 21 | 2.87 | 0.0 | 15.50 | 13.83 | 0.0 | 54.72 | 0.0 | 0.66 | 0.0960 | 0.0057 |

Table II Analysis of propeller of Table I at the design condition.

| | | | | |
|---------------|-----------|-----------------|--------------|------------------|
| V = 161.33 | DT = 5.75 | BHP = 70.00 | CP = 0.0402 | SOLIDITY = 0.058 |
| RPM = 2400.00 | DM = 1.00 | THRUST = 207.45 | CT = 0.0498 | AF = 113.92 |
| J = 0.701 | B = 2 | ALT = 0.0 | ETA = 0.8693 | DBETA = 0.0 |

| I | R | CHORD | BETA | PHI | CL | L/D | RN | MACH | A | AP |
|----|------|--------|-------|-------|--------|-------|------|------|--------|--------|
| 1 | 0.50 | 0.3353 | 56.42 | 54.75 | 0.7000 | 59.56 | 0.44 | 0.18 | 0.0333 | 0.0626 |
| 2 | 0.62 | 0.3966 | 50.50 | 48.83 | 0.7000 | 64.02 | 0.56 | 0.20 | 0.0435 | 0.0533 |
| 3 | 0.74 | 0.4325 | 45.48 | 43.81 | 0.7000 | 67.42 | 0.67 | 0.22 | 0.0525 | 0.0452 |
| 4 | 0.86 | 0.4484 | 41.24 | 39.57 | 0.7000 | 69.92 | 0.77 | 0.24 | 0.0601 | 0.0383 |
| 5 | 0.97 | 0.4501 | 37.64 | 35.97 | 0.7000 | 71.78 | 0.84 | 0.26 | 0.0663 | 0.0326 |
| 6 | 1.09 | 0.4423 | 34.57 | 32.90 | 0.7000 | 73.15 | 0.90 | 0.29 | 0.0715 | 0.0280 |
| 7 | 1.21 | 0.4285 | 31.94 | 30.27 | 0.7000 | 74.15 | 0.94 | 0.31 | 0.0757 | 0.0241 |
| 8 | 1.33 | 0.4110 | 29.66 | 27.99 | 0.7000 | 74.85 | 0.97 | 0.33 | 0.0792 | 0.0210 |
| 9 | 1.45 | 0.3913 | 27.68 | 26.01 | 0.7000 | 75.32 | 0.99 | 0.36 | 0.0821 | 0.0183 |
| 10 | 1.57 | 0.3704 | 25.95 | 24.28 | 0.7000 | 75.56 | 1.00 | 0.38 | 0.0845 | 0.0162 |
| 11 | 1.69 | 0.3487 | 24.42 | 22.75 | 0.7000 | 75.61 | 1.01 | 0.41 | 0.0865 | 0.0143 |
| 12 | 1.81 | 0.3265 | 23.06 | 21.39 | 0.7000 | 75.51 | 1.00 | 0.43 | 0.0882 | 0.0128 |
| 13 | 1.92 | 0.3040 | 21.85 | 20.18 | 0.7000 | 75.20 | 0.99 | 0.46 | 0.0897 | 0.0114 |
| 14 | 2.04 | 0.2810 | 20.77 | 19.10 | 0.7000 | 74.66 | 0.96 | 0.48 | 0.0909 | 0.0103 |
| 15 | 2.16 | 0.2572 | 19.79 | 18.12 | 0.7000 | 73.88 | 0.93 | 0.51 | 0.0920 | 0.0093 |
| 16 | 2.28 | 0.2324 | 18.90 | 17.23 | 0.7000 | 72.78 | 0.88 | 0.53 | 0.0929 | 0.0085 |
| 17 | 2.40 | 0.2059 | 18.10 | 16.43 | 0.7000 | 71.25 | 0.82 | 0.56 | 0.0937 | 0.0078 |
| 18 | 2.52 | 0.1768 | 17.36 | 15.69 | 0.7000 | 69.08 | 0.73 | 0.58 | 0.0945 | 0.0071 |
| 19 | 2.64 | 0.1433 | 16.69 | 15.02 | 0.7000 | 65.83 | 0.62 | 0.61 | 0.0951 | 0.0066 |
| 20 | 2.76 | 0.1006 | 16.07 | 14.40 | 0.7000 | 60.28 | 0.45 | 0.64 | 0.0956 | 0.0061 |
| 21 | 2.88 | 0.0 | 15.50 | 13.83 | 0.0 | 64.59 | 0.0 | 0.66 | 0.0961 | 0.0056 |